Published in final edited form as:

IEEE Trans Biomed Eng. 2008 February ; 55(2): 478–484. doi:10.1109/TBME.2007.912658.

Analysis of First-Derivative Based QRS Detection Algorithms

Natalia M. Arzeno,

Department of Electrical Engineering and Computer Science, Massachusetts Institute of Technology, Cambridge, MA 02139 USA. She was recipient of an NIH undergraduate research training award HL075014-01S1 and graduate research training award HL079503-02S1. (e-mail: natalia2@mit.edu)

Zhi-De Deng, and

Department of Electrical Engineering and Computer Science and the Department of Physics, Massachusetts Institute of Technology, Cambridge, MA 02139 USA. (e-mail: zzzdeng@mit.edu)

Chi-Sang Poon [Fellow, IEEE]

Harvard-MIT Division of Health Sciences and Technology, Massachusetts Institute of Technology, Cambridge, MA 02139 USA. (e-mail: cpoon@mit.edu)

Abstract

Accurate QRS detection is an important first step for the analysis of heart rate variability. Algorithms based on the differentiated ECG are computationally efficient and hence ideal for real-time analysis of large datasets. Here, we analyze traditional first-derivative based squaring function (Hamilton-Tompkins) and Hilbert transform-based methods for QRS detection and their modifications with improved detection thresholds. On a standard ECG dataset, the Hamilton-Tompkins algorithm had the highest detection accuracy (99.68% sensitivity, 99.63% positive predictivity) but also the largest time error. The modified Hamilton-Tompkins algorithm as well as the Hilbert transform-based algorithms had comparable, though slightly lower, accuracy; yet these automated algorithms present an advantage for real-time applications by avoiding human intervention in threshold determination. The high accuracy of the Hilbert transform-based method compared to detection with the second derivative of the ECG is ascribable to its inherently uniform magnitude spectrum. For all algorithms, detection errors occurred mainly in beats with decreased signal slope, such as wide arrhythmic beats or attenuated beats. For best performance, a combination of the squaring function and Hilbert transform-based algorithms can be applied such that differences in detection will point to abnormalities in the signal that can be further analyzed.

Index Terms

Electrocardiography; Heart rate variability; Hilbert transform; Peak detection

I. Introduction

Automatic detection of the QRS complex is necessary for efficient extraction of beat-to-beat intervals (RR) from long electrocardiogram (ECG) recordings such as nighttime data or 24-hour Holter monitoring. Accuracy of the RR series is crucial for reliable heart rate variability (HRV) analysis, which is widely considered to provide a simple noninvasive and quantitative assessment of cardiac-autonomic function in health and in disease states [1,2]. Over the past decade, HRV analysis has been increasingly recognized as a useful tool for understanding autonomic regulation during sleep [3,4] as well as patient screening in obstructive sleep apnea syndrome (OSAS) [5-7], congestive heart failure [8-11] and other disorders. However, ECG recordings may contain spurious episodes due to various disturbances such as noise interference, sudden changes in QRS amplitudes, or muscle and electrode artifacts etc., which

are not often detected correctly [12]. Studies have shown that even a single artifact in the RR signal could impart substantial spurious variance into all commonly analyzed frequency bands including those associated with respiratory sinus arrhythmia, thus motivating the need for a reliable QRS detector with minimal detection error [13].

Though many approaches exist for QRS detection, first-derivative-based methods are often used in real-time analysis or for large datasets since they do not require extensive computations. These methods also have the advantage of not necessitating manual segmentation of data, training of the algorithms, or patient-specific modifications that are often required for other detection methods [12]. However, a previous study comparing real-time detection methods showed that avoiding a delay in the detection increases the detection error [14,15]. We therefore focused on first-derivative-based methods that are designed to maximize detection accuracy instead of processing speed. Finally, although the use of multiple recording leads could improve detection accuracy especially when combined with multiple adaptive components in the detection algorithm [16], we chose to benchmark cost-effective detection algorithms that are applicable to single-lead ECG recordings.

One of the most popular single-lead first-derivative-based QRS detection methods is the Hamilton-Tompkins algorithm [17], which is an improved variation of that originally proposed by Pan and Tompkins in 1985 [18] that uses a patient-specific threshold for QRS peak detection. The Pan-Tompkins algorithm has been found to have a higher accuracy for various beat morphologies than other traditional real-time methods developed before 1990 [19]. The Hamilton-Tompkins algorithm has been widely used in the past two decades for HRV analysis for a variety of applications such as detection of OSAS in children [6], compression for optimal transmission and storage for ECG analysis [20], etc. More recently, a Hilbert transform-based method was proposed by Benitez et. al. [21] as an improved first-derivative-based QRS detection method by using a variable threshold that does not need to be experimentally determined. This method has since been employed in applications such as detecting sleep stages in patients with OSAS [22] and as a classifier for patients with paroxysmal atrial fibrillation [23]. Since the Hamilton-Tompkins algorithm and the Hilbert transform-based algorithm have been used for diverse applications, it is necessary to compare their performances under similar test conditions.

In this study, we analyzed the theoretical basis of the Hilbert transform-based algorithm and evaluated its advantages as compared to a detection algorithm that uses an additional differentiation stage as an odd filter. We then introduced an adaptive threshold to the Hamilton-Tompkins algorithm similar to that used for the Hilbert transform-based algorithm in order to eliminate the need for human intervention for the determination of the patient-specific threshold. The final goal of this study was to determine the ideal algorithm for distinguishing different classes of ECG anomalies by quantitatively comparing the various QRS detection methods and delineating their failure instances.

II. QRS Detection Algorithms

Before obtaining the first derivative of the QRS complex the ECG was bandpass filtered with a Kaiser Window filter with passband 8-20 Hz to remove baseline wander and high-frequency noise. Differentiating the ECG modifies its phase, creating zero-crossings in the location of the R-peaks. Thus a transformation is required to rectify the phase in order to create a signal with outstanding peaks in the location of the R-peaks. The algorithms described below approach the rectification stage in different ways.

A. Method I: Hilbert transform with automatic threshold

Mathematically, the Hilbert transform is defined as:

$$y(t)=\frac{1}{\pi}\int_{-\infty}^{\infty} v_r(\alpha)\frac{1}{t-\alpha}d\alpha\,, \tag{1}$$

where $v_r(t)$ is the input (e.g. the differentiated ECG). In the frequency domain, the signal is transformed with a filter of response:

$$H(e^{j\omega})=\begin{cases} -j, & 0<\omega<\pi \\ j, & -\pi<\omega<0 \end{cases}\,. \tag{2}$$

From (2), the input signal $v_r(t)$ is equivalently processed with an all-pass filter with -90° shift for positive frequencies and +90° shift for negative frequencies. The Hilbert transform is the imaginary part of the analytic signal that has the input as its real part. Fig. 2b illustrates the Hilbert transform of a differentiated ECG segment.

Because the Hilbert transform is an odd filter, the zero-crossings of the differentiated ECG, which correspond to the R-peaks, will be represented as peaks in the output of the transform. In previous studies [21,24], the effects of the Hilbert transform on the differentiated ECG have been explained in terms of its odd symmetry property and signal envelope. The Hilbert transform's all-pass characteristic prevents unnecessary signal distortion, in contrast to the second derivative method which tends to attenuate the signal at the lower frequencies (see Section II.E below). Thus, the odd-phase component of the filter provides the necessary rectification of the differentiated ECG signal in order to identify the QRS peaks while the uniform magnitude of the filter ensures that necessary information of the QRS complexes is preserved. The effects of the magnitude and phase of this transform are further explained in Section III.

The structure of the algorithm is illustrated in Fig. 1a. The differentiation of the ECG was implemented as a center differentiation stage as used by Benitez et. al. [24]:

$$v_r[n]=\frac{1}{2}(x[n+1]-x[n-1]). \tag{3}$$

Though (3) represents a non-causal filter, the three-point center derivative creates a delay of only one sample.

The algorithm was implemented in MATLAB, by which constructing the analytic signal with corresponding real part ($v_r[n]$), and taking the imaginary part as the Hilbert signal.

The variable threshold is determined automatically based on the root mean squared (RMS) value of the data segment. The RMS value of the 1024-point segment is calculated, and if it is larger than 18% of the maximum value, the threshold is set to be 39% of the maximum value of the segment. If the maximum value is in turn larger than twice the maximum value of the previous segment, the threshold is set to 39% of the maximum value of the previous segment. If the RMS of the segment is less than 18% of its maximum value, the threshold is set to 1.6 times the RMS value. The rules for determining the threshold of segment *i* are illustrated in (4).

$$\text{thresh}(i)=\begin{cases} 0.39\max(i) & ,\ \text{RMS}(i)>0.18\max(i)\&\max(i)\le 2\max(i-1) \\ 0.39\max(i-1) & ,\text{RMS}(i)>0.18\max(i)\&\max(i)>2\max(i-1) \\ 1.6\text{RMS}(i) & ,\text{RMS}(i)<0.18\max(i) \end{cases} \tag{4}$$

Once a peak is detected, the largest amplitude within a 200-ms window (set by the refractory period of a heartbeat) in the vicinity of each identified peak is stored for further analysis. A

search-back mechanism identifies the real peak in the ECG within ± 10 samples of the detected peak in the transform output.

B. Modified Method I: Hilbert transform with secondary threshold

Modified Method I has the same structure as Method I except for the introduction of a secondary threshold. Based on the secondary threshold implemented by Hamilton and Tompkins [17], the modified Method I has a secondary threshold of 0.9 times the current threshold and was applied to the intervening time segment (between 2 peaks detected by the primary threshold) when the current R-R interval exceeded 1.5 times the previous value. This secondary threshold is typically higher than that of the Hamilton-Tompkins algorithm (Section II.C.) due to the linear scale, since the differences in slope are less marked than in Method II where the squaring function magnifies any differences in slope.

C. Method II: Squaring function with patient-specific threshold

The Hamilton-Tompkins algorithm [17,18] applies a squaring function to rectify the differentiated ECG. The squaring function provides further attenuation of other ECG features, leaving the QRS complexes as outstanding positive peaks in the signal regardless of their polarity in the original ECG recording. The transform can also be viewed as a measure of energy with a threshold that verifies if the output is enough to carry the energy of a QRS complex [15]. The major disadvantage of this approach is that by squaring the differentiated ECG, normal QRS peaks with small magnitude and wide arrhythmic peaks with decreased slope are reduced in the output of the transform.

The differentiation formula as implemented in the original method is:

$$v_r[n]=\frac{1}{8}(2x[n]+x[n-1]-x[n-3]-2x[n-4]). \tag{5}$$

The five-point derivative prevents high-frequency noise amplification [25]; in the present implementation high-frequency noise is further attenuated by the Kaiser Window filter. The differentiated signal is squared ($y[n]=v_r[n]^2$) and then time-averaged by taking the mean of the previous 32 points. Peaks are found by comparing the time-averaged signal to a primary threshold, derived from the threshold coefficient and the amplitude of previous peaks. The threshold coefficients are determined in accordance with those used in Hamilton and Tompkins's study, which are specific to the MIT-BIH arrhythmia database. Application of the algorithm to other databases would require judicious selection of the ideal coefficients.

Once a peak of the time-averaged signal is detected, a search-back for the real peak in the filtered ECG is initiated from a succeeding point at half of the peak value in the time-averaged signal, with a search window of 250 ms-125 ms backward in order to account for the time shift caused by the differentiation, time-averaging, and detection scheme. After an R-peak is identified a T-wave discriminator is applied 200-360 ms later to avoid the detection of T-waves as QRS complexes. Finally, if the current RR interval is 1.5 times the previous RR interval, a secondary threshold of 0.5 times the previous threshold is set for the intervening time segment to find any missed peaks. Ideally, the threshold is set for each record on a per-patient basis though customarily (as in [17]) a universal threshold is often used instead to minimize the total error for all records in the database, sacrificing accuracy for convenience. Figure 1b illustrates the algorithm stages.

D. Modified Method II: Squaring function with automatic threshold

Next, we extended the Hamilton-Tompkins algorithm to include an automatic adjustment of the primary threshold in order to obviate subjective choice of threshold coefficients. The

modified algorithm employs the squaring function as the main transformation as with the Hamilton-Tompkins algorithm. However, time-averaging of the squared signal is not performed since it is not necessary, would require additional computations, and would introduce an unnecessary time shift in the transform output. Pan and Tompkins [18] introduced this step to extract additional information from the QRS complex but modified Method II aims at the detection (rather than characterization) of QRS complexes.

For ease of comparison, modified Method II uses the same differentiation formula as in the original Hamilton-Tompkins algorithm (5); however the thresholding mechanism is structured differently (Fig. 1a). Specifically, the square-transformed signal is subjected to a moving 1024-point window and compared to a variable thresholding rule similar to that presented previously for the Hilbert transform-based algorithm [24]. In addition, the search-back stage for modified Method II includes a T-wave discriminator as in Method II. Finally, a secondary threshold is applied as necessary to detect any missed peaks as described in Method II.

E. Method III: Second derivative of the ECG with automatic threshold

Method III was implemented in a structure similar to that described in Section II.A (see Fig. 1a). The first differentiation stage was a center derivative (3). The second differentiation stage was a forward derivative, which creates a one-sample delay and preserves most of the energy at the high frequencies corresponding to the QRS complex:

$$y[n]=v_r[n+1]-v_r[n] \tag{6}$$

The second differentiator stage ($D(e^{j\omega})$) presents a filter with odd phase and high-pass frequency response:

$$D(e^{j\omega})=e^{j\omega}-1 \tag{7}$$

$$|D(e^{j\omega})|=\sqrt{2-2\cos(\omega)} \tag{8}$$

This method rectifies the signal by its odd-phase property, resulting in a large local minimum at each QRS complex. The odd-phase and high-pass filter properties of the second differentiation stage results in non-uniform filtering of the low and high frequency components of the differentiated ECG. However, since the ECG has already been low-pass filtered, additional filtering by this method will further attenuate the QRS complexes. The smaller amplitude of this transform output can be seen in Fig. 2e. Method III thus provides a test for determining if the previous success of the Method I as a peak detector was due to the uniform magnitude or odd-phase characteristics of the Hilbert transform (see Section II.A).

III. Algorithm Comparison

The above QRS detection algorithms were tested on 48 ECG recordings from the MIT-BIH Arrhythmia Database [26]. These 30-minute recordings were sampled at 360 Hz with 11-bit resolution over a 10 mV range. Episodes of ventricular flutter in Record 207 were excluded from the analysis. A summary of the algorithmic parameters is shown in Table I. Each algorithm was applied to the bandpass-filtered and differentiated ECG. The rules for threshold determination and application of the secondary threshold can be found in Section II. The search-back range indicates the ECG or filtered ECG segment that was searched for the true location of the R-peak.

A. Overall performance of algorithms

The performance of the algorithms was affected by the characteristics of the ECG such as ectopic beats, QRS polarity, and noise level. The algorithms were compared by calculating the number of false positives (FP), true positives (TP) and false negatives (FN) for each record [27]. The sensitivity (Se) and positive predictivity (+P) of each method were calculated as follows:

$$\text{Sensitivity} = \frac{\text{TP}}{\text{TP}+\text{FN}}, \tag{9}$$

$$\text{Positive predictivity} = \frac{\text{TP}}{\text{TP}+\text{FP}}. \tag{10}$$

The average time error between the real and detected peaks was calculated as [9]:

$$\text{Average Time error (ms)} = \frac{\sum |\text{Detected QRS time} - \text{Actual QRS time}|}{\text{TP}} \tag{11}$$

As shown in Table II, Method III had the largest FP and FN values but smallest average time errors. Application of the secondary threshold in the modified version of Method I caused higher FP (78) but lower FN (-182) incidents compared with the original Method I, with a net decrease (-104) in overall false detections. Methods II and modified II had the best sensitivity and positive predictivity (Se and +P >99.5%). The RMS-based threshold determination used in the modification to Method II allowed comparable performance as Method II while eliminating the need for manual determination of the patient-specific threshold coefficient.

In Table III, |Se < 99%| and |+P < 99%| represent the number of poorly detected records with Se and +P below 99%; Min Se and Min +P show the corresponding worst-case Se and +P values. Specific records with low Se or +P are characterized in Section III.C. Method II and modified Method II had comparable worst-case scenarios. For the Hilbert transform-based algorithm inclusion of a secondary threshold (in the modified Method I) did not significantly improve detection for individual patients since the total number of poorly detected records with low Se and +P were the same for Method I and modified Method I (n = 10 each). Method III yielded the poorest results with the largest number of poorly detected records and with worst-case Se and +P values both below 90%.

B. Comparison of overall performance of algorithms

The Hilbert transform-based algorithm originally proposed by Benitez et al. was reported to yield a Se and +P as high as 99.81% and 99.83% [21] or 99.94% and 99.93% [24] on the MIT/BIH arrhythmia database. However, a recent study [23] found a Se and a +P of only 98.5% and 98.4% respectively when the Hilbert transform-based algorithm was tested on the same database. The present Hilbert transform-based algorithm (Method I) yielded a lower error rate than that of [23] but did not reach the accuracy levels reported in [21,24]. The discrepancies can possibly be caused by the use of different filter orders or different ways of calculating the Hilbert transform in the various studies. The use of a secondary threshold in the modified Method I allows the detection of peaks that were slightly below threshold. As a result, FN and the total detection errors decreased significantly even though FP increased slightly due to more T-waves and noise being misdetected as beats.

Method II produced the largest time error mainly because its search-back procedure locates the peak of the bandpass filtered ECG signal instead of the original ECG signal like the other algorithms. The non-zero phase filter in Method II shifted the peak location in the filtered ECG

to the end of the original QRS complex. This time delay of Method II is a disadvantage. By contrast, modified Method II has the disadvantage of slightly lower accuracy but the advantage of not requiring an experimentally-determined threshold. Hamilton and Tompkins [17] suggested that the threshold coefficient should be in a range of 0.15 to 0.4 for best performance, yet the ideal coefficient varies with the specific ECG recording. In addition, the modification to Method II decreased the average time error of Method II by approximately two standard deviations (Table II), whereas the difference in average time error between Method I, modified Method I, modified Method II and Method III is not significant. Consequently, Method II and modified Method II offer a tradeoff between accuracy and convenience.

Method III incurred most of the same errors as Method I and in addition yielded more than double the FN. To determine if the additional errors were caused by differences in the magnitude or phase characteristics of these methods, two new transforms were created and tested. The first transform combined the magnitude of Method I and the phase of Method III whereas the second transform combined the magnitude of Method III and the phase of Method I. The first transform, an all-pass filter with odd, linear phase, had similar results to Method I. The second transform, a high-pass filter with the phase of the Hilbert transform yielded more errors than Method I but less errors than Method III. Together, these findings suggest that the high-pass filter component of Method III was the cause of the increased error rate and that an all-pass filter, such as the Hilbert transform, provided better detection. Furthermore, the exact shape of the phase component is not important so long as the odd-phase characteristic is conserved.

C. Instances of failure

The algorithms failed at specific instances in the ECG recordings. Possible reasons for failures included:

1. False-negative detection of QRS complexes with decreased slope
    a. wide premature ventricular contractions (PVCs)
    b. low-amplitude QRS complexes
2. False-positive detection of other ECG features
    a. negative QRS complexes
    b. low signal-to-noise ratio

1) Detection of QRS complexes with decreased slope—The advantage of the secondary threshold (applied in modified Method I, Method II, and modified Method II) was evident in the presence of wide peaks, corresponding to arrhythmic beats. Figure 3 shows examples of the transform outputs of the various algorithms for normal beats and ectopic beats and the corresponding thresholds for Record 208. Methods I and III failed to detect the PVCs in the plotted record fragment. The amplitude difference between the normal beats and the PVCs was largest for Method III which produced the highest FN. Examination of the relative amplitudes of the normal beats and PVCs in Method II and modified Method II shows the necessity for the secondary threshold in these methods since the PVCs are attenuated by the squaring function. The secondary threshold in the modified Method I, set at 90% of the original threshold, was sufficiently low to detect the PVCs without false detection of noise in the segment. The secondary threshold for modified Method I, Method II, modified Method II (Fig. 3c, 3d, 3e) allowed for the detection of more PVCs than the other algorithms, though they did not achieve perfect detection. For ectopic beats with multiple peaks, the dominating peak was detected as the location of the QRS peak in agreement with the common beat indexing practice in Physionet.

Figure 3 also illustrates the delay introduced by the filter in Method II and modified Method II, where the peaks in the transform output are shifted and one preceding beat is delayed into the selected segment.

Low-amplitude QRS complexes were mainly found in one record. The resulting decreased slope created attenuated peaks at the transform output. The low-amplitude QRS complexes were successfully detected with a secondary threshold in a similar manner as the PVCs.

2) Detection of other ECG features—Accurate detection for Method I, modified Method I, and Method III was impaired by QRS complexes with reversed polarity. The phase rectification procedure for these algorithms (the Hilbert transform and differentiation) was dependent on the initial direction of the QRS complexes and thus those with reversed polarity would only be detected when the Q- or S-waves created large enough peaks in the transform output. Figure 4 illustrates this directional dependence where the R-peaks in Methods I and modified Method I (Fig. 4b, 4c) are represented as local minima compared to a positive threshold, and those in Method III (Fig. 4f) produced positive local maxima tested against a negative threshold. By contrast, the squaring function in Method II and modified Method II produced positive peaks at the transform output regardless of the polarity of the QRS complex (Fig. 4d, 4e).

Low SNR increases the number of false positives in all the algorithms. Without the secondary threshold, Method II and modified Method II had near-perfect detection for these records since the noise was greatly attenuated by the squaring function. With the use of a secondary threshold, Method II and modified Method II had higher FPs similar to the other algorithms. Figure 4 illustrates a noisy segment and the corresponding transform outputs, where the arrows point to false detections and the horizontal lines represent the threshold. The linear scale of Method I, modified Method I, and Method III (Fig. 4b, 4c, 4f) produced several noise peaks above threshold, even though some of the peaks had already been discarded by the 200-ms refractory window. The secondary threshold is not present for this segment in the modified Method I (Fig. 4c) yet its application to the previous parts of the record resulted in a lower threshold and an additional FP in the segment. The effect of the secondary threshold is again seen in the modified Method II (Fig. 4e) where two additional FPs are found. However, since all algorithms performed similarly for these datasets, the results suggest the secondary threshold did not present a significant disadvantage to Method II and modified Method II for ECG recordings with low SNR.

Since the algorithms are all based on the first derivative of the ECG, wide beats and small QRS complexes present the major detection challenge. The secondary threshold resolves some of the discrepancies in modified Method I, Method II, and modified Method II without presenting a major disadvantage in signals with high noise content. Only two records in this study were characterized with low +P due to noise mistaken as beats, yet additional steps could be taken to correct these FPs. For example, an additional stage could be introduced that compares the amplitude of the detected beat with the previous detected R peaks in the ECG. In addition, recordings with the above-mentioned features not detected correctly by the present algorithms will have beat-to-beat interval plots with outstanding peaks. Such extraneous beats can be removed manually by an expert or automatically with a procedure similar to the removal of arrhythmic beats. Finally, a combination of algorithms which have different transform properties and detection attributes (such as modified Method I and modified Method II) can be performed on each record such that any discrepancies thereof can be further scrutinized for artifacts.

IV. Conclusion

All the algorithms presented in this study except Method III resulted in Se and +P above 99%. Method II, the Hamilton-Tompkins algorithm had the lowest detection error but the highest average time error. Although the variation to the Hamilton-Tompkins algorithm, modified Method II, yielded a slightly increased error rate, it obviated the need for an experimentally determined threshold coefficient. The success of the Hilbert transform-based method was ascribable in part to the odd-phase component of the filter but more importantly, to its uniform magnitude spectrum. The modification to Method I, introducing a secondary threshold, slightly improved accuracy for the Hilbert transform-based method.

For all the algorithms, the detection errors arose from a variety of factors including the existence of wide premature ventricular contractions, low-amplitude peaks, peaks with reversed polarity, and signals with low SNR. The application of an automatically adapted threshold in modified Method I, Method II, and modified Method II allows these accurate, computationally simple algorithms to be used for real-time applications and the processing of large databases. A combination of Method I or modified Method I and modified Method II can also be used as a first-pass or online detection system such that artifacts can be identified by comparison of the results from these algorithms for further analysis by an expert.

Acknowledgements

This work was supported by National Institutes of Health Grants HL075014 and HL079503.

References

1. Malliani A, et al. Cardiovascular neural regulation explored in the frequency domain. Circulation 1991;84(2):482–492. [PubMed: 1860193]
2. Task Force of the European Society of Cardiology and the North American Society of Pacing and Electrophysiology. Heart rate variability: standards of measurement, physiological interpretation, and clinical use. Circulation 1996;93(5):1043–1065. [PubMed: 8598068]
3. Scholz UJ, et al. Vegetative background of sleep: spectral analysis of the heart rate variability. Physiology & Behavior 1997;62(5):1037–1043. [PubMed: 9333197]
4. Trinder J, et al. Autonomic activity during human sleep as a function of time and sleep stage. J Sleep Res 2001;10(4):253–264. [PubMed: 11903855]
5. Penzel T, et al. Systematic comparison of different algorithms for apnoea detection based on electrocardiogram recordings. Med Biol Eng Comput 2002;40(4):402–407. [PubMed: 12227626]
6. Zapanta L, et al. Heart rate chaos in obstructive sleep apnea in children. IEEE Trans Eng Med Biol 2004:3889–3892.
7. Shouldice RB, et al. Detection of obstructive sleep apnea in pediatric subjects using surface lead electrocardiogram features. Sleep 2004;27:784–792. [PubMed: 15283015]
8. Guzzetti S, et al. Different spectral components of 24 h heart rate variability are related to different modes of death in chronic heart failure. Eur Heart J 2005;26(4):357–362. [PubMed: 15618038]
9. Jiang W, et al. Ability of heart rate variability to predict prognosis in patients with advanced congestive heart failure. Am J Cardiol 1997;80(6):808–811. [PubMed: 9315600]
10. Poon CS, Merrill C. Decrease of cardiac chaos in congestive heart failure. Nature 1997;389:492–495. [PubMed: 9333237]
11. Kearney MT, et al. Predicting sudden death in patients with mild to moderate chronic heart failure. Heart 2004;90(10):1137–1143. [PubMed: 15367507]
12. Kohler BU, Hennig C, Orlgmeister R. The principles of software QRS detection. IEEE Trans Eng Med Biol Mag 2002;21(1):42–57.
13. Berntson G, Stowell J. ECG artifacts and heart period variability: Don't miss a beat! Psychophys 1998;32:127–132.

14. Paoletti M, Marchesi C. Discovering dangerous patterns in long-term ambulatory ECG recordings using a fast QRS detection algorithm and explorative data analysis. Comput Methods Programs Biomed 2006;82(1):20–30. [PubMed: 16529841]
15. Suppappola S, Sun Y. Nonlinear transforms of ECG signals for QRS detection: A Quantitative Analysis. IEEE Trans Eng Biomed Eng 1994;41(4):397–400.
16. Christov I. Real time electrocardiogram QRS detection using combined adaptive threshold. Biomed Eng Online 2004;3(1):28. [PubMed: 15333132]
17. Hamilton PS, Tompkins WJ. Quantitative investigation of QRS detection rules using the MIT/BIH arrhythmia database. IEEE Trans Eng Biomed Eng 1986;12:1157–1165.
18. Pan J, Tompkins W. A real-time QRS detection algorithm. IEEE Trans Eng Biomed Eng 1985;32(3): 230–236.
19. Portet F, Hernandez AI, Carrault G. Evaluation of real-time QRS detection algorithms in variable contexts. Med Biol Eng Comput 2005;43(3):379–85. [PubMed: 16035227]
20. Peiró MM, et al. FPGA custom DSP for ECG signal analysis and compression. Lecture Notes in Computer Science 2004:954–958.
21. Benitez DS, et al. A new QRS detection algorithm based on the Hilbert transform. Comput Cardiol 2000;27:379–382.
22. Redmond SJ, Heneghan C. Cardiorespiratory-based sleep staging in subjects with obstructive sleep apnea. IEEE Trans Biomed Eng 2006;53(3):485–496. [PubMed: 16532775]
23. Hickey B, Heneghan C, De Chazal P. Non-episode-dependent assessment of paroxysmal atrial fibrillation through measurement of RR interval dynamics and atrial premature contractions. Annals of Biomed Eng 2004;32(5):677–687.
24. Benitez DS, et al. The use of the Hilbert transform in ECG signal analysis. Comput Biol Med 2001;31:399–406. [PubMed: 11535204]
25. Ligtenberg A, Kunt M. A robust-digital QRS-detection algorithm for arrhythmia monitoring. Comput Biomed Res 1983;16(3):273–86. [PubMed: 6872535]
26. Goldberger AL, et al. PhysioBank, PhysioToolkit, and PhysioNet: components of a new research resource for complex physiologic signals. Circulation 2000;101(3):e215–e220. [PubMed: 10851218]
27. Association for the Advancement of Medical Instrumentation. American national standard for ambulatory electrocardiographs, publication ANSI/AAMI EC38-1994. 1994

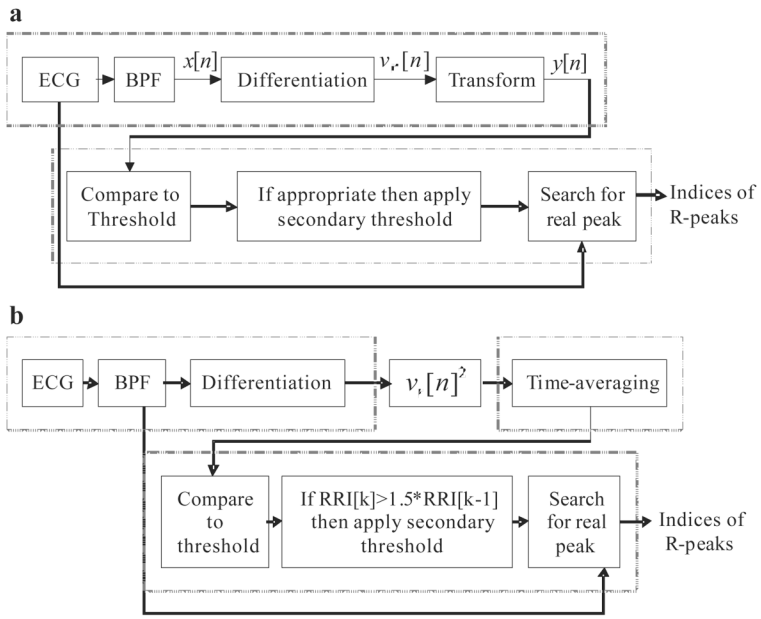

Fig. 1.

Algorithm structures. (a) Structure for Method I, modified Method I, modified Method II, and Method III. (b) Structure for Method II.

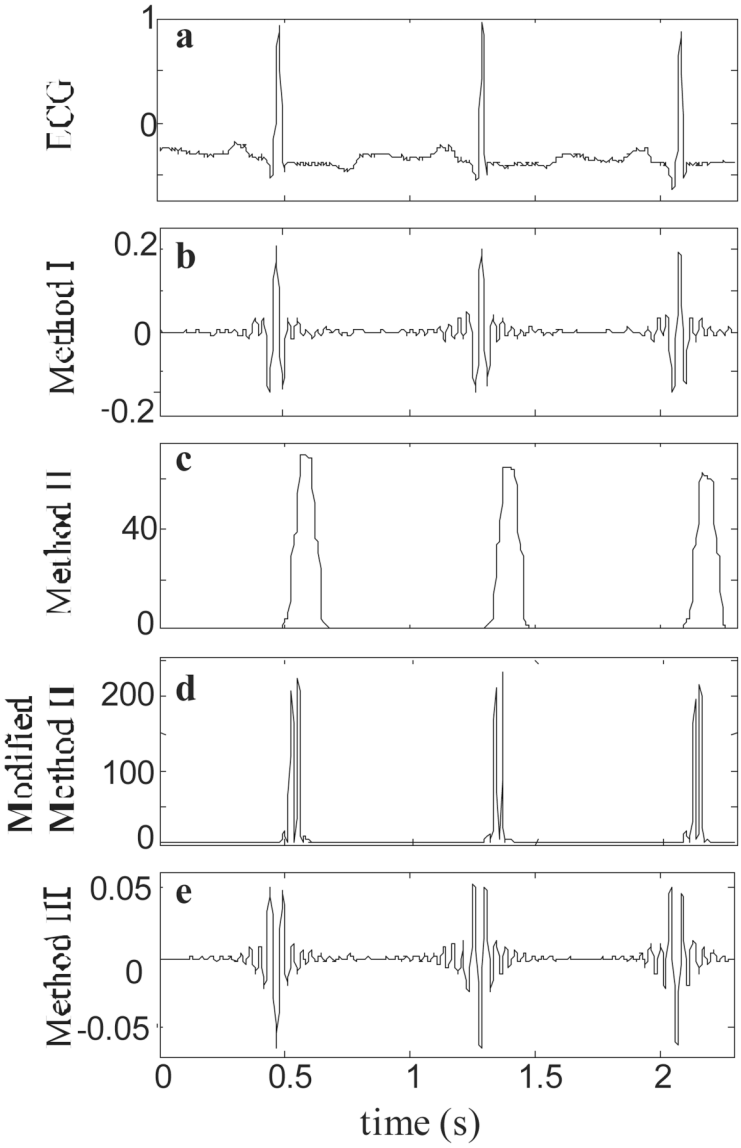

Fig. 2.
Output of transforms.

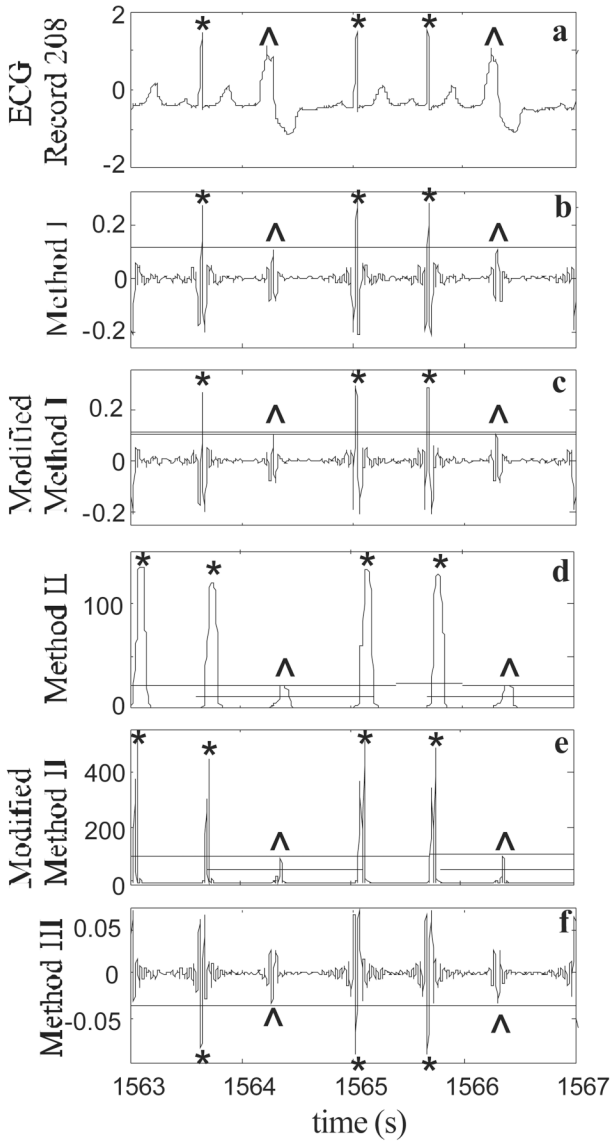

Fig. 3.

PVC in Record 208. A segment of the original ECG and the outputs of the transforms are plotted. The * signals a normal beat and the ˆ signals a PVC. The horizontal lines in the transform outputs show where the threshold was set. The lower lines in modified Method I, Method II, and modified Method II represent the secondary threshold.

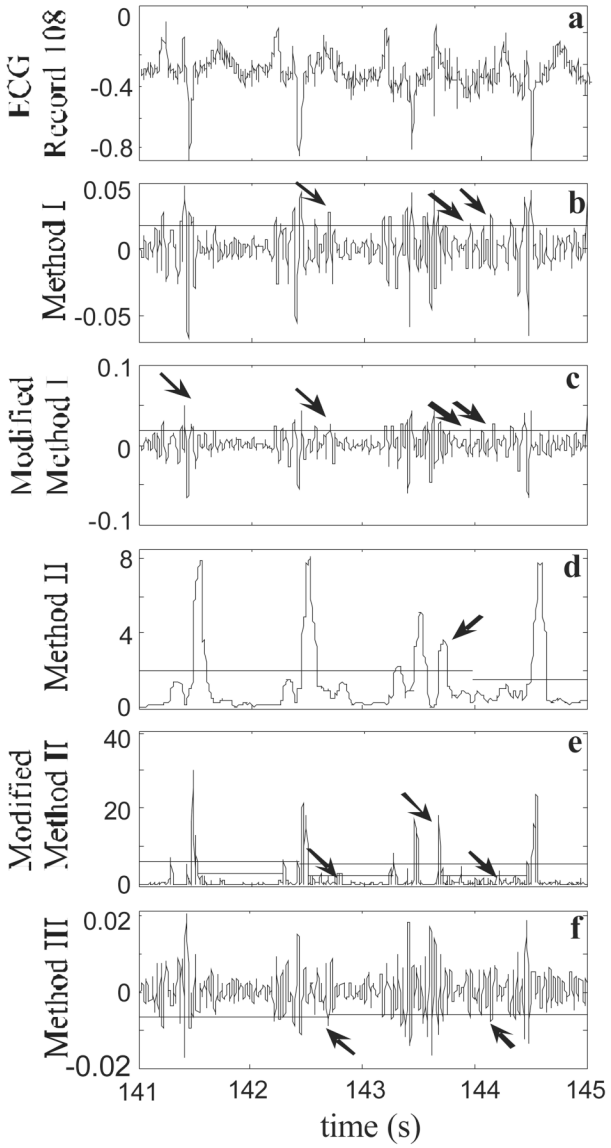

Fig. 4.

Reversed polarity QRS complexes and high noise content in Record 108. The output of the transforms for the different algorithms are plotted, where the arrows point to FPs and the horizontal lines represent the threshold.

TABLE I

Summary of Algorithms

Method	Transform	Threshold Determination	Secondary Threshold	Search-back range
I	Hilbert Transform	Based on RMS of segment	None	+/- 10 points from peak detection in ECG
I (modified)	Hilbert Transform	Based on RMS of segment	0.9 times threshold	+/- 10 points from peak detection in ECG
II	Squaring and Time-averaging	Threshold coefficient times predicted peak value	0.5 times threshold	250-125ms prior to peak detection in BPF
II (modified)	Squaring	Based on RMS of segment	0.5 times threshold	+/- 10 points from peak detection in ECG
III	Differentiation	Based on RMS of segment	None	+/- 10 points from peak detection in ECG

TABLE II

Cumulative Results for Peak Detection

Method	FP	FN	TP	Se (%)	+P (%)	Avg. Time Error (SD) (ms)
I	758	957	108499	99.13	99.31	7.00 (8.1)
I (modified)	836	775	108681	99.29	99.24	7.08 (8.1)
II	405	354	109099	99.68	99.63	55.82 (20.2)
II (modified)	447	467	108989	99.57	99.59	7.90 (4.9)
III	884	2112	107344	98.07	99.18	6.50 (7.6)

TABLE III

Worst-Case Sensitivity and Positive Predictivity

Method	|Se < 99%|	Min Se (%)	|+P < 99%|	Min +P (%)
I	10	93.75	10	89.00
I (modified)	10	95.76	10	88.20
II	5	97.08	6	95.53
II (modified)	6	96.24	8	95.17
III	16	80.24	10	86.51